THE ASTROPHYSICAL JOURNAL, 378:326–346, 1991 September 1

ASTEROSEISMOLOGY OF THE DOV STAR PG 1159−035 WITH THE WHOLE EARTH TELESCOPE

D. E. WINGET,[1,2] R. E. NATHER,[1] J. C. CLEMENS,[1] J. PROVENCAL,[1] S. J. KLEINMAN,[1] P. A. BRADLEY,[1] M. A. WOOD,[1] C. F. CLAVER,[1] M. L. FRUEH,[1] A. D. GRAUER,[3,4] B. P. HINE,[5] C. J. HANSEN,[6] G. FONTAINE,[7] N. ACHILLEOS,[8] D. T. WICKRAMASINGHE,[8] T. M. K. MARAR,[9] S. SEETHA,[9] B. N. ASHOKA,[9] D. O'DONOGHUE,[10] B. WARNER,[10] D. W. KURTZ,[10] D. A. BUCKLEY,[10] J. BRICKHILL,[10] G. VAUCLAIR,[11] N. DOLEZ,[11] M. CHEVRETON,[12] M. A. BARSTOW,[13] J. E. SOLHEIM,[14] A. KANAAN,[15,16] S. O. KEPLER,[15,17] G. W. HENRY,[18] AND S. D. KAWALER[19]

Received 1990 June 15; accepted 1991 March 5

ABSTRACT

We report the results from 264.1 hr of nearly continuous time-series photometry on the pulsating pre-white dwarf star (DOV) PG 1159−035. The high-resolution power spectrum of this data set is dominated by power in the range from roughly 1000 to 2600 μHz (1000 s to 385 s periods). This power is completely resolved into 125 individual frequencies; we have identified 101 of them with specific, quantized pulsation modes, and the rest are completely consistent with such modal assignment. The luminosity variations are therefore certainly the result of g-mode pulsations. Although the amplitudes of some of the peaks exhibit significant variations on time scales of a year or so, the underlying frequency structure of the pulsations is stable over much longer intervals.

With the help of existing linear theory we use these identifications to determine, or strongly constrain, many of the fundamental physical parameters describing this star. We find its mass to be 0.586 $M_{\odot}$, its rotation period 1.38 days, its magnetic field less than 6000 G, its pulsation and rotation axes to be aligned, and its outer layers to be compositionally stratified. With straightforward extensions of existing theory it may be possible to determine uniquely from this data set *all* of the parameters necessary to construct a quantitative model of its interior.

These observations also reveal several interesting phenomena that challenge the current theory of nonradial pulsations, and may require substantial new developments to describe them.

Subject headings: stars: individual (PG 1159−035) — stars: pulsation — stars: white dwarfs

[1] Department of Astronomy and McDonald Observatory, University of Texas, Austin, TX 78712.
[2] Alfred P. Sloan Research Fellow.
[3] Department of Physics and Astronomy, University of Arkansas, 2801 South University Avenue, Little Rock, AR 72204.
[4] Visiting Astronomer, Kitt Peak National Observatory.
[5] NASA Ames Research Center, M.S. 244-4, Moffett Field, CA 94035.
[6] Joint Institute for Laboratory Astrophysics, University of Colorado, Box 440, Boulder, CO 80309.
[7] Departement de Physique, Université de Montréal, C.P. 6128, Succ. A. Montréal, Quebec H3C 3J7, Canada.
[8] Department of Mathematics, Australian National University, Canberra, Australia.
[9] Indian Space Research Organization, Technical Physics Division, ISRO Satellite Center, Airport Road, Bangalore 560 017, India.
[10] Department of Astronomy, University of Cape Town, Rondebosh 7700, Cape Province, South Africa.
[11] Observatoire Midi-Pyrenees, 14 Avenue E. Belin, 31400 Toulouse, France.
[12] Observatoire de Paris-Meudon, F-92195 Meudon, Principal Cedex, France.
[13] Physics Department, University of Leicester, Leicester LE1 7RH, UK.
[14] Institutt for Matematiske Realfag, Universitet i Tromso, 9000 Tromso, Norway.
[15] Instituto de Fisica, Universidade Federal do Rio Grande do Sul, 90049 Porto Alegre-RS, Brazil.
[16] Visiting Astronomer, Laboratorio Nacional de Astrofisica, CNP, Brazil.
[17] Visiting Astronomer, Cerro Tololo Inter-American Observatory.
[18] Center of Excellence in Information Systems, Tennessee State University, 330 10th Avenue, North, Nashville, TN 37203.
[19] Department of Physics and Astronomy, Iowa State University, Ames, IA 50211.

1. INTRODUCTION

Determining the basic physical parameters of white dwarf stars is one of the most potentially rewarding problems in astrophysics; success would enable us to map out the evolution of the stellar population of the Galaxy. We could measure the age of the disk as well as the halo in a self-consistent way, and investigate the detailed history of star formation in the galaxy (see the recent review by Wood 1990, and references therein).

Winget et. al. (1987) and subsequent investigators (e.g., Iben & Laughlin 1989) have shown that the ages of the coolest white dwarf stars provide an accurate measure of the age of the Galactic disk, and that the shape of the observed luminosity function contains detailed information about the history of star formation there. White dwarf cooling theory forms a stable basis for this work: Winget & Van Horn (1987) demonstrated that, if the basic physical parameters of the theoretical models are agreed upon by the various investigators involved, there is excellent quantitative agreement among them regarding the theoretical age and luminosity relations, and hence the age and chronology of the disk.

Knowledge of the basic physical parameters of individual white dwarf stars would also help us understand their progenitors. Information about stellar masses, envelope structures, and rotation rates, were they available, would show us the results of the extensive mass-loss stages preceding white dwarf

formation, and perhaps reveal the role of nuclear shell burning in this process.

The new field of asteroseismology offers a way to determine these important physical parameters: it is the study of stellar structure and evolution as revealed by global stellar oscillations. The oscillations provide a view beneath the photosphere, and contain information about basic stellar parameters such as mass, composition, layering, rotation period, magnetic field strength, temperature, and luminosity. The clarity of this view is directly related to the number of oscillations present and clearly resolved in the time-series spectra.

It was the discovery of the rich global oscillations in the Sun that led to the development and refinement of this technique (termed helioseismology when applied to the Sun). Its application to white dwarf stars is extremely promising: except for the Sun, the number of individual frequencies observed in pulsating white dwarfs is greater than that for any other kind of pulsating star (Unno et al. 1989). Solar oscillations are very small in amplitude—similar effects in nearby Sunlike stars have been sought with very limited success—so we can detect them only because we live very near their source. In contrast, oscillations in white dwarfs are much larger and more readily measured: as much as 30% of the total light can be modulated. Pulsating white dwarfs offer a large variety of targets for testing our theoretical understanding of stellar interiors.

This study, and others to follow, will test the machinery of asteroseismology—the theory of nonradial pulsations—in many cases for the first time. In the process we can hope to measure directly, or at least constrain, the fundamental parameters of the pulsating white dwarf and pre-white dwarf stars. Because these pulsators are otherwise normal stars (see Winget 1988a and references therein) these parameters will pertain to the entire class of white dwarfs and the stars that form them.

The amount of asteroseismological information available is a sensitive function of the number of fully resolved pulsation modes. Unfortunately, as the number of modes increases above a handful—beyond which the powerful tools of asteroseismological analysis become most useful—it becomes impossible to unravel the light curve into its component frequencies from a single observing site. The regular daytime gaps, and the less regular gaps from weather, combine to produce alias frequencies in the Fourier transforms of the time-series data which become hopelessly entangled with the real power.

We have solved this basic observational problem by developing a global, interactive network of photometric observers who together provide essentially continuous coverage of a set of prioritized targets. We call this network the Whole Earth Telescope (hereafter WET). The operation of this new instrument, and the basic techniques we have developed for analyzing the extended time-series data it provides, are described by Nather et al. (1990).

2. THE PULSATING DOV STAR PG 1159−035

Since its discovery (McGraw et al. 1979) the hot, oscillating DOV pre-white dwarf star PG 1159−035 (GW Vir, McGraw's star) has been the object of intense study. *EXOSAT* observations of its X-ray spectrum placed its surface temperature in the range 123,000–124,000 K (Barstow et al. 1986; Barstow & Holberg 1989), which is too high to permit hydrogen lines to show in its optical spectrum; He II λ4686 was seen in absorption. Estimates of its surface gravity ($\log g \approx 7$) by Wesemael, Green, & Liebert (1985) indicate it has not yet fully contracted onto the white dwarf cooling sequence.

The Fourier transform of its time-series behavior from earlier studies indicated several "bands" of power—groups of distinct frequencies that were unresolved in even the combined light curve obtained from two different longitudes (Winget 1988a). Those observations (Winget et al. 1985) did demonstrate, however, that one of the peaks in the power spectrum, at a period of 516 s, apparently had no close companions in frequency and was therefore stable in period and phase; they were able to measure its secular rate of period change, dP/dt, and show that its value was consistent with that predicted by cooling theory. Kawaler (1986, 1987a, b, 1988) was able to constrain the spherical harmonic index of the mode, l, to be either 1 or 3, and then used an approximate period spacing to derive a mass for the star. Later observations (Koupelis & Winget 1987; Winget & Kepler 1988) showed that new bands of power had appeared in the power spectrum where none had been visible before.

We selected PG 1159−035 as our primary target for the WET run in 1989 March. We were reasonably confident that the pulsations were nonradial g-modes because their observed periods were too long to be radial modes, and Barstow et al. (1986) were able to demonstrate approximate phase coherence between X-ray and optical pulsations of the same frequency. The identification of the pulsations as g-modes, based partly on analogies with other much cooler classes of pulsating white dwarf stars, was not completely certain, however; particularly disquieting was the theoretical requirement for very high radial overtones, of order 20 to 50, to match the observed periods.

This paper describes the results of our first investigation of this star with the Whole Earth Telescope during 1989 March.

3. DATA ACQUISITION AND REDUCTION

The specific composition of the WET varies from run to run depending on the declination of the target objects; in this case, the near-equatorial declination of PG 1159−035 allowed observatories in both hemispheres to participate in the observations. We list them in Tables 1, and, in Table 2, we present a journal of the 264.1 hr of high-speed photometric observations used in our analysis of this star. All sites were equipped with two-star photometers (although the second channel was not operational at the Sutherland site) except the Australian observatory, which had the Montreal three-star photometer, and the 1.9 m telescope of Haute Provence, which used the Chevreton three-star photometer. Integration times were 10 s for all of the individual runs. The details of our data reduction procedure are presented in Nather et al. (1990); we summarize them here.

Both three-star photometers used the third channel for continuous observation of the sky background. For these data, we subtracted the sky on a point by point basis. In all the other data, we interrupted the observations of the target and comparison star for about 1 minute of sky observations at irregular intervals of roughly 20 minutes (when the Moon was up and the sky was very bright) to 1 hr (a more typical value since the bulk of the observations were obtained during dark-time). We then interpolated linearly between sky observations and subtracted the result from the data.

As a test, we also used a spline fit to the sky readings and found no significant difference in the reduced data, and so chose to use the simpler linear fits. The effects of extinction and other slow transparency variations were accounted for by fitting a third-order polynomial to each sky-subtracted data set

TABLE 1

PARTICIPATING SITES

Observatory	Location	W. Longitude (hr)	Latitude	Telescope (m)
McDonald	Mount Locke, Texas	6.9	+30°40′	2.1
U. of Hawaii	Mauna Kea, Hawaii	10.4	+19 49	0.6
Siding Spring	Siding Spring Mt., N.S.W.	14.1	−31 16	1.0
Vainu Bappu	Kavalur, India	18.8	+12 34	1.0
SAAO[a]	Sutherland, South Africa	22.6	−32 22	0.8
Haute-Provence	St. Michel, France	23.6	+43 56	1.9
Roque de los Muchachos	La Palma, Canary Islands	1.2	+28 46	2.5
LNA[b]	Itajubá, Brazil	3.0	−22 31	1.9
CTIO[c]	Cerro Tololo, Chile	4.7	−30 10	1.5

[a] South African Astronomical Observatory.
[b] Laboratorio Nacional de Astrofisica.
[c] Cerro Tololo Interamerican Observatory.

TABLE 2

JOURNAL OF OBSERVATIONS

Run Name	Telescope	Date (UT)	Start (UT)	Length (s)
JCC-0072	Siding Spring 1.0 m	1989 Mar 1	12:14:00	18960
JCC-0074	Siding Spring 1.0 m	1989 Mar 2	12:13:00	23600
SN4527	SAAO 0.8 m	1989 Mar 2	18:52:00	29500
REN-0059	La Palma 2.5 m	1989 Mar 2	23:07:20	24070
MLF-0006	McDonald 2.1 m	1989 Mar 3	4:45:27	16490
S4528	SAAO 08 m	1989 Mar 3	20:58:00	7400
REN-0061	La Palma 2.5 m	1989 Mar 3	23:08:20	18470
TOL-0003	CTIO 1.5 m	1989 Mar 4	3:35:00	20520
JCC-0075	Siding Spring 1.0 m	1989 Mar 4	11:26:30	27020
S4531	SAAO 0.8 m	1989 Mar 4	18:35:00	30500
TOL-0005	CTIO 1.5 m	1989 Mar 5	2:29:00	24450
JCC-0076	Siding Spring 1.0 m	1989 Mar 5	11:10:00	28000
S4532	SAAO 0.8 m	1989 Mar 5	18:35:01	29200
K40-0042	Kavalur 1.0 m	1989 Mar 5	18:37:40	17470
TOL-0007	CTIO 1.5 m	1989 Mar 6	2:13:30	25410
REN-0065	La Palma 2.5 m	1989 Mar 6	2:42:00	10570
JCC-0077	Siding Spring 1.0 m	1989 Mar 6	12:44:10	15290
K40-0050	Kavalur 1.0 m	1989 Mar 6	15:50:35	4100
K40-0051	Kavalur 1.0 m	1989 Mar 6	17:00:00	20170
JCC-0078	Siding Spring 1.0 m	1989 Mar 6	17:01:20	6620
S4533	SAAO 0.8 m	1989 Mar 6	18:46:00	20540
REN-0068	La Palma 2.5 m	1989 Mar 7	0:42:37	6360
TOL-0009	CTIO 1.5 m	1989 Mar 7	2:21:00	25370
MLF-0013	McDonald 2.1 m	1989 Mar 7	8:59:39	10350
JCC-0080	Siding Spring 1.0 m	1989 Mar 7	11:21:30	25650
S4534	SAAO 0.8 m	1989 Mar 7	18:37:04	31320
TOL-0011	CTIO 1.5 m	1989 Mar 8	2:19:00	25050
MLF-0014	McDonald 2.1 m	1989 Mar 8	4:42:41	25180
A123	Mauna Kea 0.6 m	1989 Mar 8	8:02:10	19610
JCC-0081	Siding Spring 1.0 m	1989 Mar 8	11:42:20	19420
S4535	SAAO 0.8 m	1989 Mar 8	18:21:01	32410
TOL-0013	CTIO 1.5 m	1989 Mar 9	2:13:00	18300
MLF-0015	McDonald 2.1 m	1989 Mar 9	4:36:09	26320
JCC-0083	Siding Spring 1.0 m	1989 Mar 9	11:05:30	26620
GV-0055	OHP 1.9 m	1989 Mar 9	22:00:00	17250
S4536	SAAO 0.8 m	1989 Mar 9	20:13:40	25300
MLF-0016	McDonald 2.1 m	1989 Mar 10	4:32:05	16890
S4537	SAAO 0.8 m	1989 Mar 10	18:51:01	30010
GV-0057	OHP 1.9 m	1989 Mar 10	21:59:10	20190
RA108	Itajuba 1.6 m	1989 Mar 11	0:58:40	24470
S4538	SAAO 0.8 m	1989 Mar 11	18:30:03	29260
GV-0059	OHP 1.9 m	1989 Mar 11	22:10:10	21140
A124	Mauna Kea 0.6 m	1989 Mar 12	7:23:30	19290
A125	Mauna Kea 0.6 m	1989 Mar 12	12:59:30	5640
S4539	SAAO 0.8 m	1989 Mar 12	22:36:01	14230
A126	Mauna Kea 0.6 m	1989 Mar 13	7:36:00	3000
A127	Mauna Kea 0.6 m	1989 Mar 13	11:01:40	13830

and then dividing by this fit. This also normalized the data, so we then subtracted 1 to give a mean of zero for all the data sets. This procedure yields a light curve with variations in amplitude as a fraction of the total intensity; such reduced light curves from different sites can then be combined without further processing. We used the data obtained on a nearby comparison star in channel 2 to measure sky transparency. Data contaminated by cloud were discarded.

The final product of these basic reduction procedures is shown in Figure 1, the light curve of the 6.5 day interval when all the observatories where on-line. Note that the overlaps—where data were obtained simultaneously at two sites at different longitude—are visible only by the increased density of points; there are no discontinuities in the light curve that arose from "stitching" the runs from individual sites into the composite whole.

4. HIGH-RESOLUTION POWER SPECTROSCOPY OF PG 1159–035

About 3 days into the WET run, the previously known bands of unresolved power in the Fourier transform began to separate into distinct peaks; after the end of the sixth day it was clear that essentially all the peaks were resolved. We applied a simple test to verify that the resolved power spectrum was stable: we divided the data into two halves and analyzed each half separately. Figure 2 shows the result. With only small differences in the power in some peaks, which arise from differing gaps in the two data sets (and therefore somewhat different sidelobe patterns) the two halves show identical spectra.

We display the spectral window—the Fourier transform pattern obtained by sampling and transforming a single sinusoid in the exactly same way the data are sampled—for the complete data set in Figure 3. The more conventional representation of the spectral window as the pattern obtained from the transform of the data window—i.e., by transforming a sampled signal of frequency 0 and amplitude 1—is generalized here by allowing the frequency and amplitude to assume other values. This procedure yields a pattern symmetrical about the chosen frequency, whose amplitudes can be matched to those in the observed data, but with exactly the same properties as the conventional spectral window. It allows us to locate the sidelobes which surround strong peaks, and to see how they add (in the complex plane) by creating synthetic power spectra with more than one (data sampled) frequency present.

The high-resolution power spectrum of the entire WET run is shown in Figure 4. It was constructed by adding together

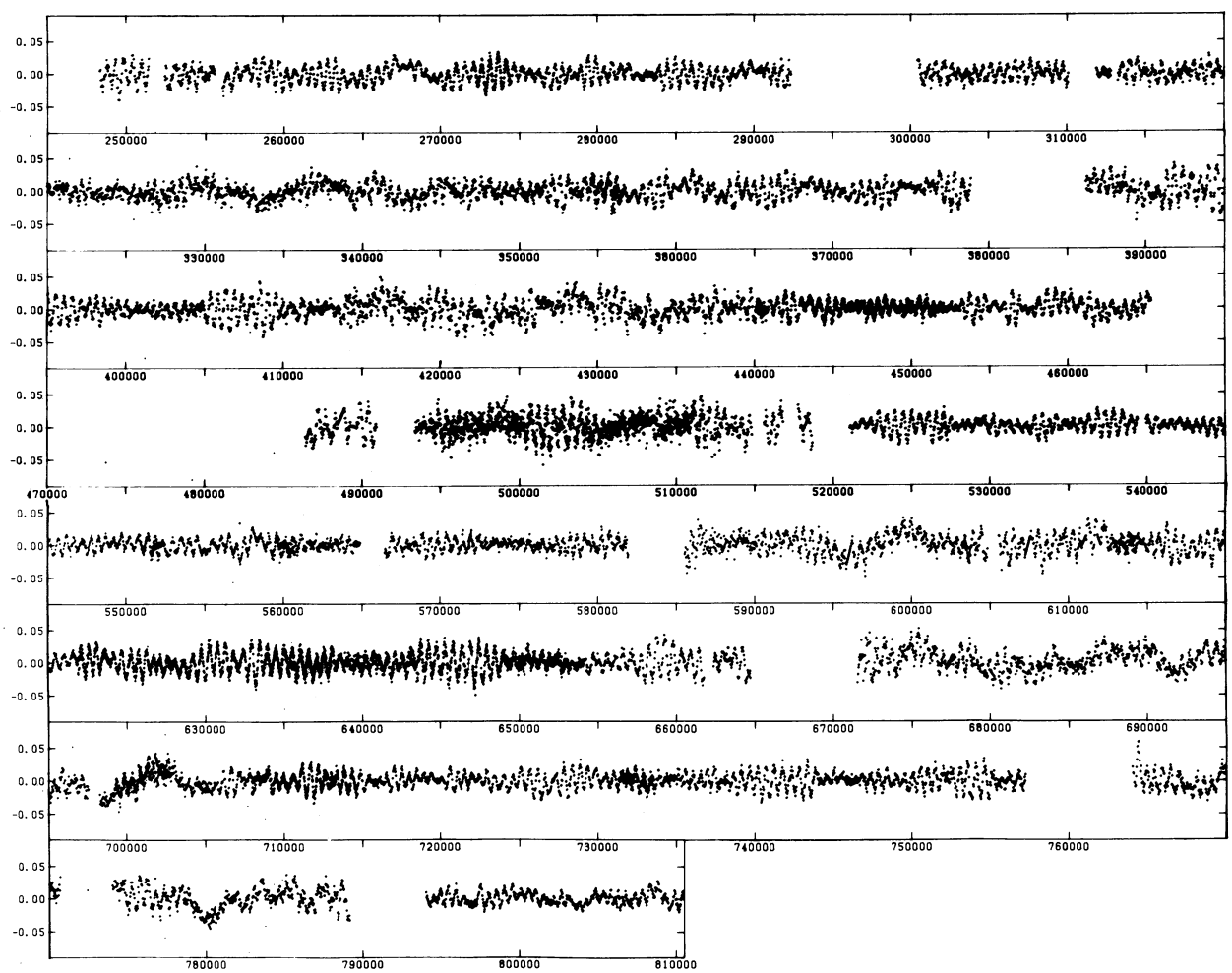

FIG. 1.—Light curve of PG 1159−035 during the central 6 days of the WET run when all the telescopes were on-line. The horizontal axis shows elapsed time in seconds, and the vertical axis shows fractional intensity.

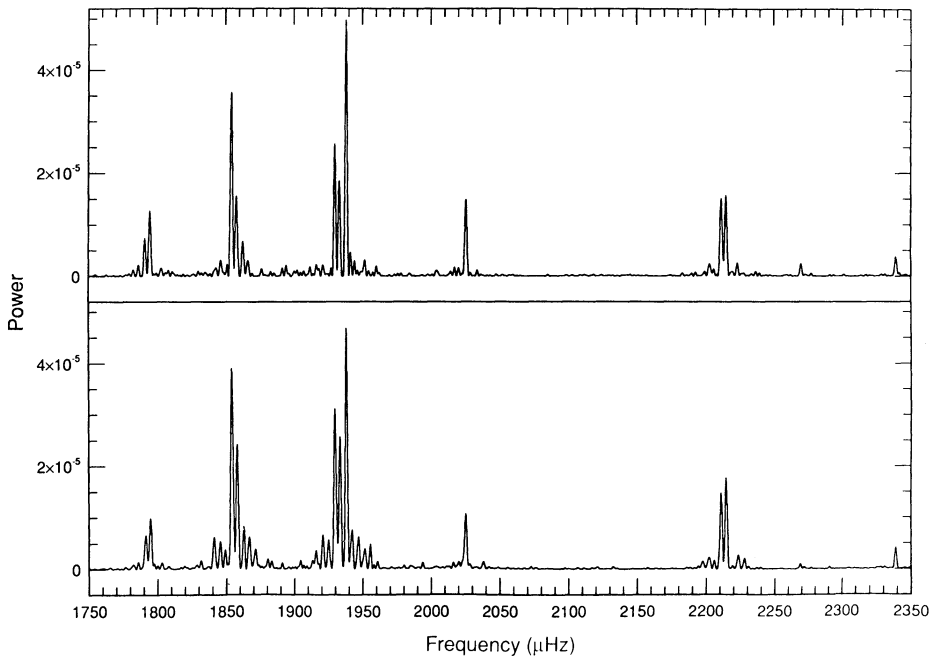

FIG. 2.—Power spectra obtained when the light curve was divided into two equal halves and processed separately. Except for small sidelobe effects arising from differing data gaps, the spectra are the same.

Fourier spectra of the individual runs into real and imaginary arrays whose size and resolution had previously been estimated from the scheduled length of the WET run (Nather et al. 1990). The noise level in the power spectrum begins to rise, roughly exponentially, below about 300 μm, thus diluting any signal that might be present, and it rolls off to zero below about 50 μHz. The latter effect is the result of the way we have reduced the data: division by polynomials removes any variations in the data, whether in the star or not, on time scales longer than typical individual runs (around 20,000 s). Any changes in the signal-to-noise ratio due to changing from one telescope to another will appear in this low-frequency region, but the effect is so small we were unable to identify it.

The peaks of greatest power in the Fourier spectrum are largely confined to the interval from 1000 to 2600 μHz, with the dominant power in the narrower interval between 1750 and 2250 μHz. Note that the vertical scale in the fourth panel in Figure 4 is over 10 times larger than the scales used in the other panels.

Most of the large-amplitude regions are now seen to divide

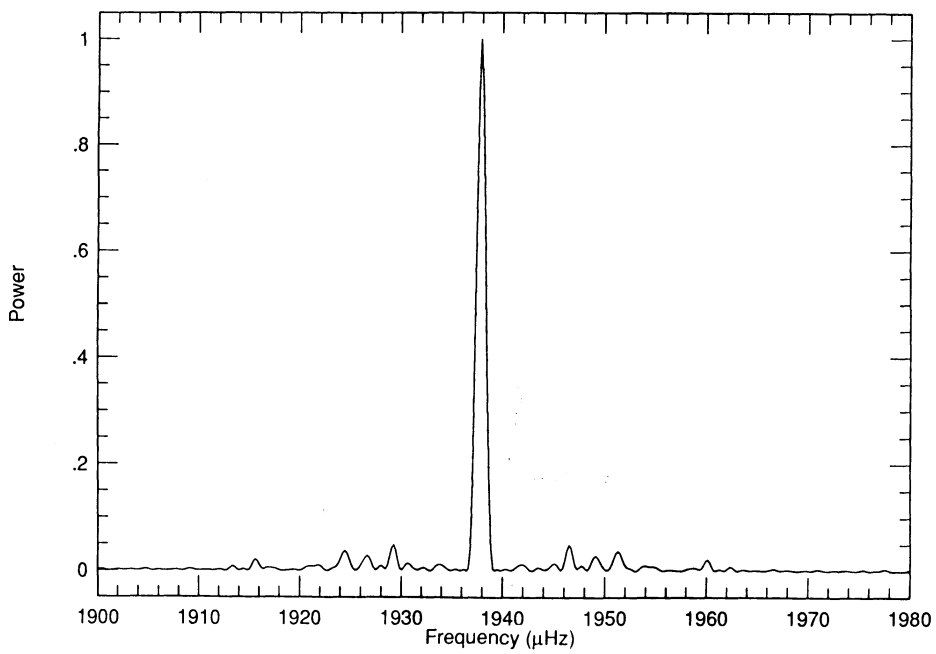

FIG. 3.—Spectral window of the complete data set, showing the patterns of peaks that results from the presence of a single frequency in the power spectrum.

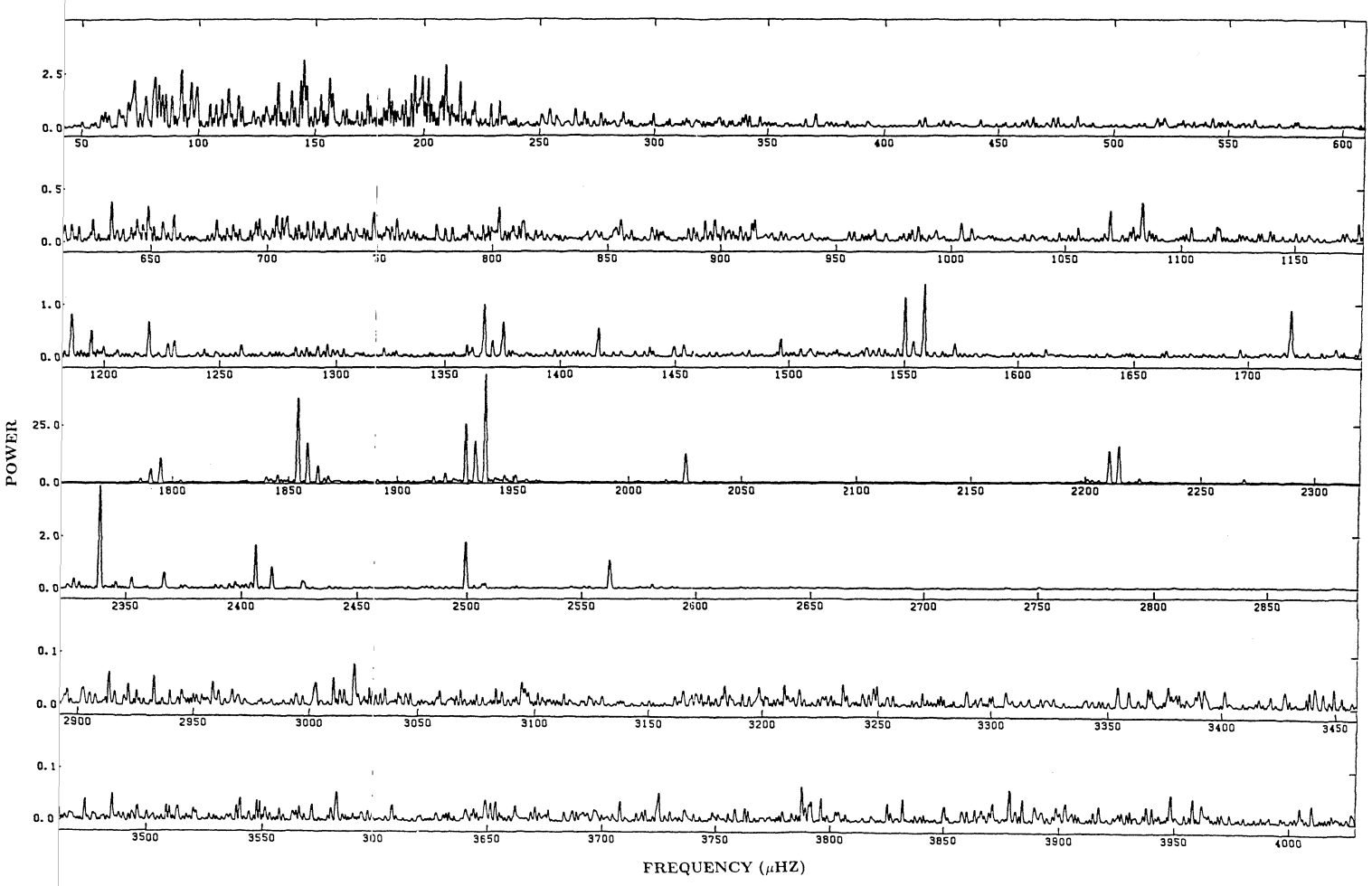

FIG. 4.—Power spectrum of the complete data set, shown as power in units of 10^{-6} vs. frequency in μHz. The vertical scale is different for each panel in an attempt to accommodate the dynamic range.

into triplets, with their members spaced uniformly in frequency; the triplets occur at approximately equal intervals in period. Similarly there are groups of 4 or 5 frequencies (most apparent in the region 2250–2600 μHz) with uniform, but somewhat larger frequency splitting. These groups also occur at approximately constant period intervals which are smaller than those of the triplets. There are no obvious multiplets that have more than five components.

Nonradial pulsation theory immediately suggests an explanation for these patterns. Each multiplet could represent a single quantized g-mode pulsation, with integer spherical harmonic index l and radial overtone number k, which has been split into the observed fine structure by rotation of the star. In the simplest case each member of a multiplet would then be one of $2l + 1$ possible pulsation modes characterized by the azimuthal quantum number m, which assumes integer values from $-l$ through 0 to $+l$.

We adopt the convention that a positive value of m represents azimuthal waves running in the same direction as the rotation of the star; that is, positive values of m represent prograde modes. We therefore associate the sign of m with the direction of wave propagation, a convention adopted by Unno et al. (1979). The major virtue of this convention is that the mode with the largest m in a multiplet ($m = l$) also has the highest frequency. Retrograde modes are represented by negative values of m.

It is tempting to suppose that the observed triplets are $l = 1$ modes and the quintuplets are $l = 2$. Such immediate identification would be premature, however, since some of the m modes may not be excited—thus triplets might also represent $l = 2$ or above. For this identification to be certain, the spacings between and within multiplets must conform to those demanded by the theory. Unno et al. (1979) show that, as a simple consequence of the asymptotic dispersion relation for g-mode pulsations, successive values of k will yield multiplet groups uniformly separated in period, provided that k is large enough. If P_{kl} is the period for a given l and k where, for the moment, we suppress any reference to m, then this dispersion relation yields

$$P_{kl} = k\,\Delta\Pi[l(l+1)]^{-1/2} + \text{constant} \equiv k\,\Delta P_l + \text{constant}\ ,$$

where $\Delta\Pi$ is a constant in the simplest examples, and its value depends only on the structure of the particular star under consideration.

As originally pointed out by Kawaler (1987a, b), the value of ΔP_l depends on the stellar mass, $M/M_\odot$, and the value of l. For models representative of the DOV stars—meaning those with essentially *any* mass within the observed range for hot white dwarf stars combined with any luminosity greater than 10 $L_\odot$—the ratio of $\Delta P_l = 1$ to $\Delta P_l = 2$ is within a few percent of its asymptotic value $\Delta P_{l=1}/\Delta P_{l=2} = \sqrt{3} \approx 1.73$. Comparison with the mean spacing between the multiplets (which will be shown to be 21.5 and 12.5 s, respectively) leaves no doubt that the triplets are indeed $l = 1$ modes and the quintuplets are $l = 2$. We will see below that these identifications are made firmer by examining the frequency splitting within each group, and confirmed by the results from the two different analytical tests described in § 5.2.

In Table 3 we have compiled a complete list of all significant peaks in the power spectrum between 1000 and 3000 μHz. The amplitudes of both signal and noise vary in this wide spectral region, so we have broken it into three ranges and have applied a different detection threshold in each. Complete identification is also made difficult in the region of large-amplitude pulsations where sidelobes resulting from the few data gaps can mimic or obscure low-amplitude pulsations. These sidelobes can combine with each other, or with real peaks, and require far more than casual inspection, or application of the (single frequency) spectral window, to ferret them out. In difficult cases we have generated an artificial power spectrum using noise-free sine waves, sampled in exactly the same way as the data, to compare with the original power spectrum and demonstrate which peaks are real and which are artifacts. We illustrate this procedure in § 5.1 below. We have identified these "alias peaks" and removed them from the listing in Table 3.

We also include peaks with amplitudes below the detection thresholds which have been tentatively identified based on frequency or period spacing constraints. These amplitudes are identified in the table with a colon. In some cases a peak is significant but its modal identification is uncertain; in this case we place the possible alternative identification for l in parentheses, and indicate the uncertainty with a colon after the assigned value for m.

For the lowest frequencies in the table, just above 1000 μHz, individual multiplets for $l = 2$ actually overlap each other and make identification uncertain. In other regions of the spectrum, patterns for $l = 1$ overlap those for $l = 2$, and are difficult to untangle. The presence of noise, and sidelobes from pulsations with large amplitudes, also add to uncertainties in identification in different regions of the spectrum. Despite these problems, however, Table 3 shows that all of the significant peaks can either be identified as, or are consistent with, patterns corresponding to either $l = 1$ or $l = 2$. We find no evidence for any pulsation that must correspond only to $l = 3$.

5. ASTEROSEISMOLOGY

We are now in a position to examine the pulsation properties in some detail, and employ the techniques of asteroseismology to give either exact determinations, or place strong constraints on the most fundamental properties of the star PG 1159−035. As we will see, this single set of observations has, in one step, both caught and surpassed our theoretical understanding of nonradial pulsation processes. We will examine three areas in which observation can confront current theory: the fine-structure splitting and its consequences, the regular period spacing and its consequences, and the rate of period change and secular evolution of the star.

5.1. *The Fine-Structure Multiplets and Rotational Splitting*

In Figure 5 we have plotted all of the readily identified multiplets in the transform on the same horizontal scale, with each multiplet displaced vertically for clarity. This figure illustrates that the fine-structure splitting between successive members of a multiplet is very nearly uniform in frequency, ν_l, for both the $l = 1$ and $l = 2$ modes. It also indicates that there is very little variation in the amount of splitting for multiplets of different frequency; this is consistent with the theoretical expectations for high values of k. If we take the average of the splittings for the modes shown in Figure 5 we find that $\langle \delta\nu_{l=1} \rangle = 4.22 \pm 0.04$ μHz, and $\langle \delta\nu_{l=2} \rangle = 6.92 \pm 0.07$ μHz. These values are independent of the manner of averaging: we tried normalizing to the total power in each multiplet, using the data unnormalized, and normalizing each to its largest

TABLE 3

PEAKS IN THE POWER SPECTRUM

Frequency (μHz)	Period (s)	Fractional Amplitude in units of 10^{-4}	l	m
1004.77.....	995.25	4.1	2, (1)	−2:
1011.81.....	988.33	2.2:	2, (1)	−1:
1018.10.....	982.22	2.4:	2, (1)	0:
1026.23.....	974.44	2.0:	2, (1)	+1:
1032.28.....	968.73	2.6:	2, (1)	+2:
1069.22.....	935.26	5.4	2, (1)	
1083.07.....	923.30	6.1	2, (1)	
1178.10.....	848.82	4.2	2, (1)	
1186.43.....	842.86	9.0	1	−1
1190.45.....	840.02	3.7:	1	0
1194.73.....	837.01	7.2	1	+1
1200.04.....	833.31	4.5	2	
1219.54.....	819.98	8.3	1	−1
1223.81.....	817.12	3.1:	1	0
1227.94.....	814.37	5.1	1	+1
1230.67.....	812.57	5.6	2	
1259.52.....	793.95	4.8	1	−1
1264.31.....	790.94	2.6:	1	0
1267.99.....	788.65	2.9:	1	+1
1282.91.....	779.48	4.4	2	
1287.58.....	776.65	4.3	1	−1
1292.38.....	773.77	4.6	1	0
1296.43.....	771.35	4.9	1	+1
1328.83.....	755.38	4.1:	1	−1
1327.80.....	753.12	2.9:	1	0
1332.55.....	750.44	2.2:	1	+1
1359.62.....	735.50	4.8	2, (1)	
1361.95.....	734.24	4.3	2, (1)	
1367.11.....	731.47	10.0	1	−1:
1370.80.....	729.50	5.6	1	0:
1375.43.....	727.05	8.1	1	+1:
1407.87.....	710.29	3.3:	1	−1
1412.59.....	707.92	2.5:	1	0
1416.59.....	705.92	7.4	1	+1
1439.10.....	694.88	4.2	2	
1449.89.....	689.71	4.3	1	−1
1454.11.....	687.71	4.8	1	0
1458.12.....	685.81	3.3	1	+1
1496.89.....	668.05	5.8	1	−1
1501.01.....	666.22	2.8:	1	0
1505.24.....	664.34	3.8:	1	+1
1533.95.....	651.91	4.1	2	
1539.24.....	649.67	4.1	2	
1547.47.....	646.22	4.0	2	
1550.39.....	645.00	10.7	1	−1
1554.23.....	643.41	5.5	1	0
1558.87.....	641.49	11.8	1	+1
1572.53.....	635.92	5.0	2	
1601.64.....	624.36	2.6:	1	−1
1606.17.....	622.60	3.0:	1	0
1609.07.....	621.48	2.1:	1	+1
1653.66.....	604.72	2.5:	1	−1
1658.25.....	603.04	1.7:	1	0
1662.66.....	601.44	2.8:	1	+1
1716.37.....	582.62	3.3:	1	−1:
1720.30.....	581.29	1.9:	1, (2)	0:
1724.24.....	579.97	1.5:	1, (2)	+1:
1719.08.....	581.71	9.5	2, (1)	−2:
1726.59.....	579.18	3.0	2	−1:
1732.59.....	577.17	3.0	2	0:
1738.74.....	575.13	3.8	2	+1:
1747.65.....	572.20	4.4	2	+2:
1749.68.....	571.53	4.4	(2)	
1786.24.....	559.84	12.9	1	−1
1790.70.....	558.44	24.6	1	0
1794.88.....	557.14	33.0	1	+1
1854.04.....	539.36	61.0	1	−1
1858.20.....	538.16	41.6	1	0
1862.58.....	536.89	27.3	1	+1
1929.32.....	518.32	51.0	1	−1
1933.55.....	517.18	42.4	1	0
1937.83.....	516.04	68.9	1	+1
2016.46.....	495.92	11.0	1	−1
2020.80.....	494.85	8.2	1	0
2025.13.....	493.80	35.6	1	+1
2124.24.....	470.76	3.5:	1	−1
2129.62.....	469.57	3.3:	1	0
2133.15.....	468.79	4.4:	1	+1
2201.27.....	454.28	12.5	(2), (1)	
2203.13.....	453.90	11.0	(2), (1)	
2205.86.....	453.34	10.8	(2), (1)	
2210.31.....	452.43	37.3	(2), (1)	
2214.38.....	451.59	40.1	1, (2)	−1:
2218.74.....	450.71	8.4	1, (2)	0:
2223.20.....	449.80	13.8	1, (2)	+1:
2269.14.....	440.70	12.7	2	−2:
2276.69.....	439.23	6.2:	2	−1:
2283.10.....	438.00	2.8	2	0:
2290.45.....	436.60	6.1	2	+1:
2321.04.....	430.84	3.4:	1	−1
2325.35.....	430.04	4.0	1	0
2330.24.....	429.14	5.1:	1	+1
2338.89.....	427.55	19.8	2	−2
2345.78.....	426.30	5.2	2	−1
2352.76.....	425.03	6.6	2	0
2359.68.....	423.79	3.2	2	+1
2366.76.....	422.52	8.0	2	+2
2406.18.....	415.60	13.1	2	−2:
2413.12.....	414.40	9.1	2	−1:
2419.54.....	413.30	3.0:	2	0:
2426.51.....	412.11	5.5	2	+1:
2499.61.....	400.06	13.4	2, (1)	
2503.29.....	399.47	3.4	2, (1)	
2506.97.....	398.89	4.4	2, (1)	
2508.14.....	398.70	4.6	2, (1)	
2521.97.....	396.52	3.2	2, (1)	
2551.23.....	391.97	3.1	2, (1)	
2562.11.....	390.30	10.4	2	−2
2568.93.....	389.27	2.1	2	−1
2576.83.....	388.07	1.8	2	0
2589.72.....	386.14	2.6	2	+2
2750.92.....	363.51	2.4	2	−2
2757.34.....	362.67	1.3	2	−1
2764.28.....	361.76	4.6	2	0
2771.78.....	360.78	0.9	2	+1
2834.96.....	352.74	2.4	2	−2
2842.14.....	351.85	2.1	2	−1
2848.89.....	351.01	1.3	2	0
2856.25.....	350.11	1.6	2	+1
2863.00.....	349.28	0.9	2	+2
2933.28.....	340.91	2.4	2	−2
2940.26.....	340.11	1.7	2	−1
2947.80.....	339.24	1.2	2	0
2953.88.....	338.54	1.5	2	+1
2961.15.....	337.71	1.7	2	+2

NOTES.—Colons (:) after amplitudes indicate modes identified by spacing constraints; after m values indicate other identifications are possible. Modes in parentheses indicate a possible alternative identification.

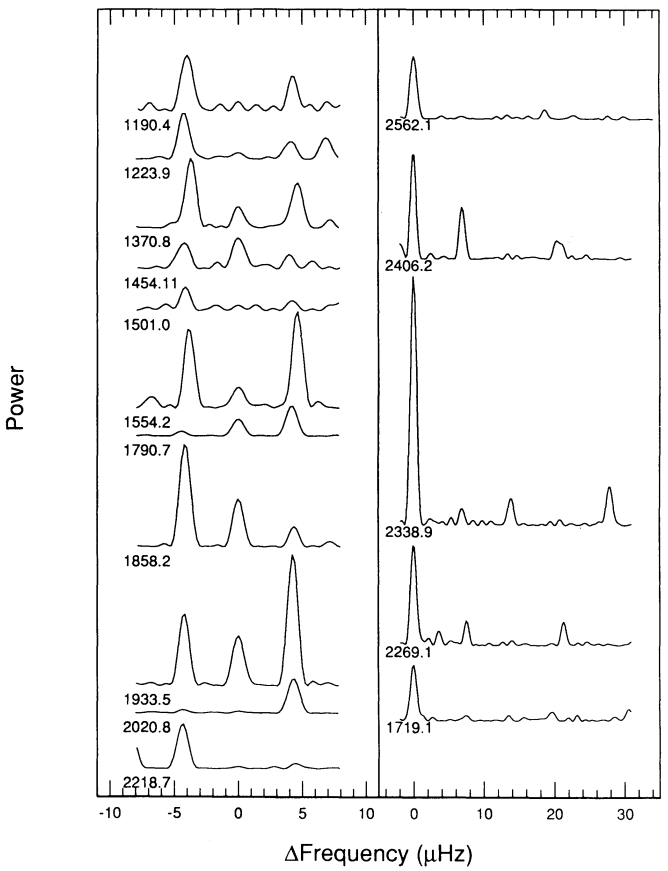

FIG. 5.—Individual multiplets for $l = 1$ (*left panel*) and for $l = 2$ (*right panel*). The number under each curve is the frequency in μHz for the $m = 0$ mode (for $l = 1$), and the $m = -2$ mode (for $l = 2$).

component; all three methods gave the same results. We can now consider the possible causes for such fine structure.

5.1.1. *The Magnetic Field*

Two different physical effects can cause frequency splitting: slow rotation or magnetic fields: either mechanism breaks the potential degeneracy in m that perfect spherical symmetry implies. The nearly uniform character of the splitting allows us to choose between them. Magnetic fields large enough to produce the observed splittings will produce only $l + 1$ modes rather than $2l + 1$ modes and, most importantly, the splitting is proportional to m^2 (Jones et al. 1989). This is clearly *not* the case for the $l = 2$ modes.

We can use the maximum deviation from uniform splitting to set a limit on the magnetic field strength. In Figure 6 we display the average multiplet profiles for $l = 1$ and $l = 2$. These represent the straight average obtained by summing over the modes shown in Figure 5. These frequency splittings are uniform to better than 5% for individual $l = 1$ modes, a value constrained by run length, implying an upper limit to the magnetic field $B < 6000$ G.

5.1.2. *The Rotation Axis and Rotation Rate*

Rotation can produce just the sort of uniform splitting of nonradial g-modes we observe (see Cox 1984 for an excellent discussion). A rotation time scale may be inferred from the observed frequency splitting as $P_{\rm rot} \sim 1/\delta\nu_l$. This yields $P_{\rm rot}$ of order days and suggests that approximations based on slow rotation should be valid; further, for the relatively large values of k we expect to be associated with our observed models, we can also assume that asymptotic limits for period spacings are valid. We can therefore derive the theoretical expectation for the ratio, $R_{l,l'}$, of the splitting interval within multiplets for l versus l' (see Appendix). We find that $R_{1,2} = 0.60$.

We can compare this number to the splitting ratio we have actually observed. We take as our best estimate the splitting in

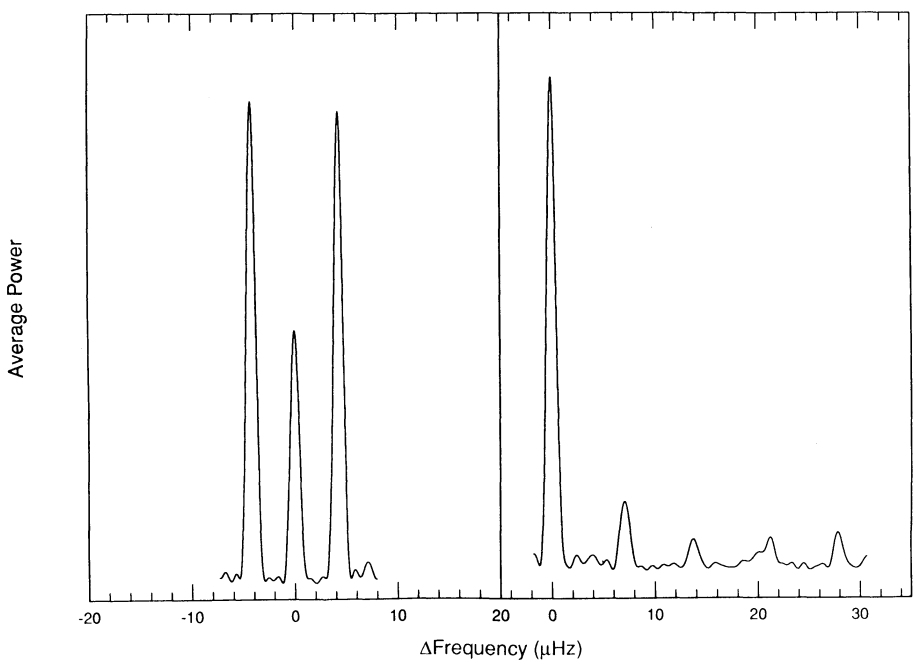

FIG. 6.—Average of the power in the multiplets shown in Fig. 4 for $l = 1$ (*left panel*) and $l = 2$ (*right panel*)

the average of each set of modes (Fig. 6):

$$R_{1,2} = \frac{\delta\nu_{l=1}}{\delta\nu_{l=2}} = \frac{4.22}{6.92} = 0.61 ,$$

which is very close to that expected from theory, and further strengthens our previous assignment of the l values.

Now we are in a position to derive, in the uniform rotation limit, a true rotation period—rather than just a rotation time scale—for the star. For uniform rotation and in the asymptotic overtone limit for k,

$$P_{\rm rot} = \frac{1 - [l(l+1)]^{-1}}{\delta\nu_l} .$$

Using the $l = 1$ value we get $P_{\rm rot} = 1.371 \pm 0.13$ days, and for $l = 2$ we get $P_{\rm rot} = 1.388 \pm 0.013$ days. If we take the average of the two periods as our best value, then the rotation period is

$$P_{\rm rot} = 1.38 \pm 0.01 \text{ days}$$

in the region of period formation.

We can, in addition, say something about the geometry of the pulsations compared to the alignment of the rotation axis. If the symmetry axis for the pulsations is not aligned with the rotation axis, then the number of possible multiplets is $[2l + 1]^2$, where the spacing in frequency between submultiplets depends on the extent of the misalignment (Pesnell 1985). Since, to within our ability to measure, we see only triplets and quintuplets, we conclude that the two axes are very closely aligned.

5.1.3. *Multiplet Amplitudes and Inclination*

The differing amplitudes we observe in a given multiplet can result from two different effects: the inclination of the pulsation axis to our line of sight, and (potentially) different amplitudes resulting from differing strengths of the intrinsic driving mechanism for different modes (e.g., Dziembowski 1988). If this latter effect is negligible, we should be able to derive the star's inclination to our line of sight from the relative amplitudes of the modes we observe.

Considering only modes with $l = 1$, the central frequency ($m = 0$) corresponds to an alternate brightening of the north and south poles of the star; if we view the star pole-on, at low inclination (0°), the whole disk would brighten and darken once per oscillation cycle. The surrounding pair of frequencies ($m = \pm 1$) correspond to waves of brightness traveling in opposite directions around the equator of the star, however, and from our pole-on view would seem to cancel out completely, since we are unable to resolve the disk, and are limited to seeing the integrated brightness changes across it. For a pole-on view, then, we would see the $m = 0$ mode at full amplitude, and would see no brightness changes resulting from the $m = \pm 1$ modes.

In contrast, if we view the same star in the plane of its equator, at high (90°) inclination, the alternate brightening of the north and south poles will cancel out, and we will see *only* the changes due to the waves of brightness running in opposite directions around its equator—so we will see the $m = \pm 1$ modes at full amplitude, and will not see the $m = 0$ mode at all. At an inclination of 45°, all three members of the triplet would appear at reduced but equal amplitudes.

Figure 5 shows clearly that the observed amplitudes in a given multiplet are *not* symmetric around the $m = 0$ mode, which implies that the amplitudes are different for different values of m. However, at least for the $l = 1$ multiplets, the *average*, as shown in Figure 6, is indeed symmetric around $m = 0$: the modes $m = -1$ and $m = +1$ have almost identical amplitudes. If differing excitation effects tend to average out, as the symmetry in Figure 6 would seem to suggest, we can then derive the inclination from the ratio of the $m = 0$ amplitude to the average of the $m = \pm 1$ modes. For the observed power ratio of 1.9 (amplitude ratio of 1.4) we find $i \approx 60°$.

Pesnell (1985) has computed the effect of inclination for various values of l, assuming the amplitudes at the stellar surface are equal for all of the modes within a multiplet. A simple interpolation of Pesnell's graphical results for $l = 1$, which include limb darkening and projection effects, also yields $i \approx 60°$.

We cannot yet assess the uncertainty associated with this result, since intrinsic differences in excitation could affect the value we derive. The very different amplitudes seen in the average power for the $l = 2$ modes suggest caution: the various amplitudes values do not average out to produce a symmetric average quintuplet—perhaps because there are fewer multiplets to average together—but the very large mean amplitude for the retrograde mode $m = -2$ implies a very large intrinsic excitation compared with its modal siblings. Current nonradial pulsation theory offers no explanation for such an effect.

5.2. *The Multiplet Separations as a Function of k*

Nonradial pulsation theory predicts that the period spacing between successive multiplets of g-modes for a given value of l will be completely uniform only if there are no density discontinuities in the stellar interior. This is a severe idealization, of course: even a pure carbon white dwarf model would show a discontinuity associated with the internal degeneracy boundary (which, in turn, strongly affects the behavior of the Brunt-Väisälä frequency), and we can expect real white dwarfs to show additional effects due to chemical layering brought about by diffusion under the effect of their strong gravitational fields.

Observed variations in spacing between multiplets of the same l for successive values of k can therefore provide a powerful diagnostic of the internal discontinuities arising from degeneracy and chemical layering. Theoretical models of the expected period spacings have been calculated by Kawaler (1986, 1987b) and by Cox (1987). We can use the variations from period spacing uniformity as a probe of internal structure, and the average spacing to derive the mass of the star.

5.2.1. *The Mass of PG 1159−035*

In order to search for uniform period spacings in an unbiased way, we took the power spectrum of the entire WET data set in the region from 1000–3000 μHz, converted the frequencies to periods, and thus derived a period transform (hereafter PT). We then computed the Fourier transform of the PT; the result is displayed in Figure 7.

We can identify only three significant peaks in the result. If we use a nonlinear least-squares technique to derive the values and errors for each one, we find peaks at 21.51 ± 0.03, at 12.67 ± 0.03, and 10.78 ± 0.03 s. The third peak is just the first harmonic of the 21.5 s peak, and arises because the narrow "pulse" shapes in the PT are very far from sinusoids, so we expect harmonics to result. Of course, the peak with the longest period in the set—which also has by far the highest amplitude—is one physically significant peak, and corresponds to the period spacing for $l = 1$. The peak at 12.7 s corresponds to the period spacing for $l = 2$. We can now use the $m = 0$

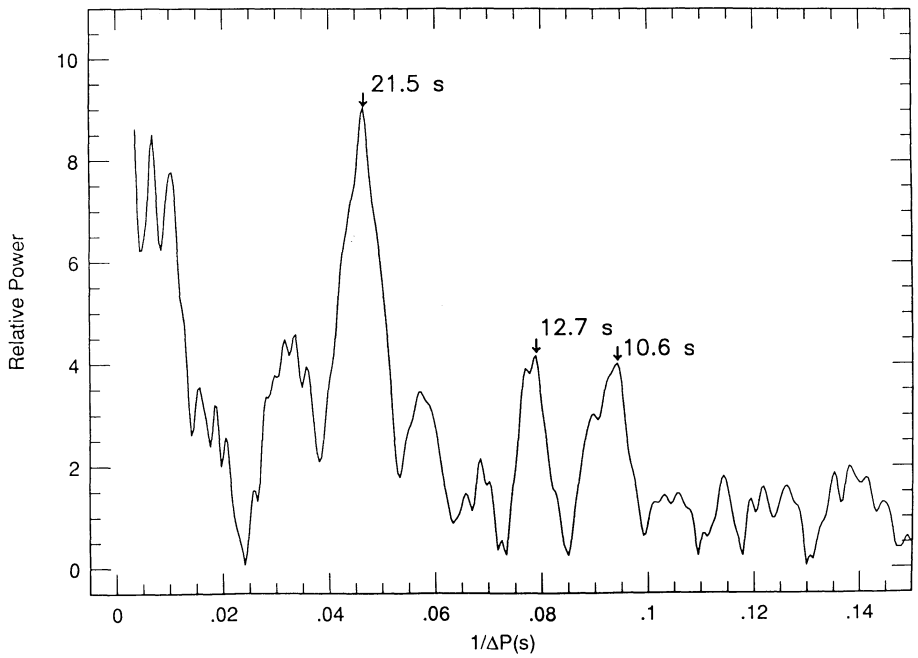

FIG. 7.—Fourier transform of the period spectrum of PG 1159−035, showing the preferred period spacing of 21.5 and 12.7 s. The peak of 10.6 s is the first harmonic of the 21.5 s peak.

spacings in Table 3 to assign $\Delta P_{l=1} = 21.5 \pm 0.03$ s and $\Delta P_{l=2} = 12.67 \pm 0.03$ s.

The advantage of the PT transform approach is that it is directly related to the observations, with no intervening interpretation. It has the disadvantage that it is not a standard technique, so we will compare these results with those of the Kolmogorov-Smirnov (KS) test (Kawaler 1988). This test, however, is less direct, in that it takes as its input the peaks we have identified (Table 3) and therefore depends to some extent on our ability to remove any spurious peaks that arise from aliases.

The result obtained by applying the KS test to the identified peaks is displayed in the lower panel of Figure 8. We have also included in the upper panel the results from Kawaler (1988) who used the earlier, and not completely resolved, time-series spectra. A comparison of the two panels illustrates the importance of obtaining very long time-series data as we do with the WET.

The KS results in the lower panel are very similar in many respects to those of the PT in Figure 7. The KS shows nearly equal minima at 21.85 and 21.05 s for $l = 1$ modes; this bifurcation arises as a result of resonant mode trapping, discussed below. The average of these two values is 21.5 s, which agrees with the results from the PT transform. Further confirmation for this value comes from a least-squares straight line fit to the $l = 1$ periods of Table 3, which yields a period spacing of 21.48 ± 0.06 s. The KS test also shows a strong minimum at 12.69 s which is consistent with the $l = 2$ mode period spacing from the PT analysis.

A complication for the $l = 2$ result from either analysis arises, however, from the very different amplitudes we measure for the members of the $l = 2$ multiplets: they will find a spacing dominated by the high-amplitude $m = -2$ member, while comparison with theory must be made for spacings between the modes with $m = 0$. Correcting for this effect yields 12.5 s for

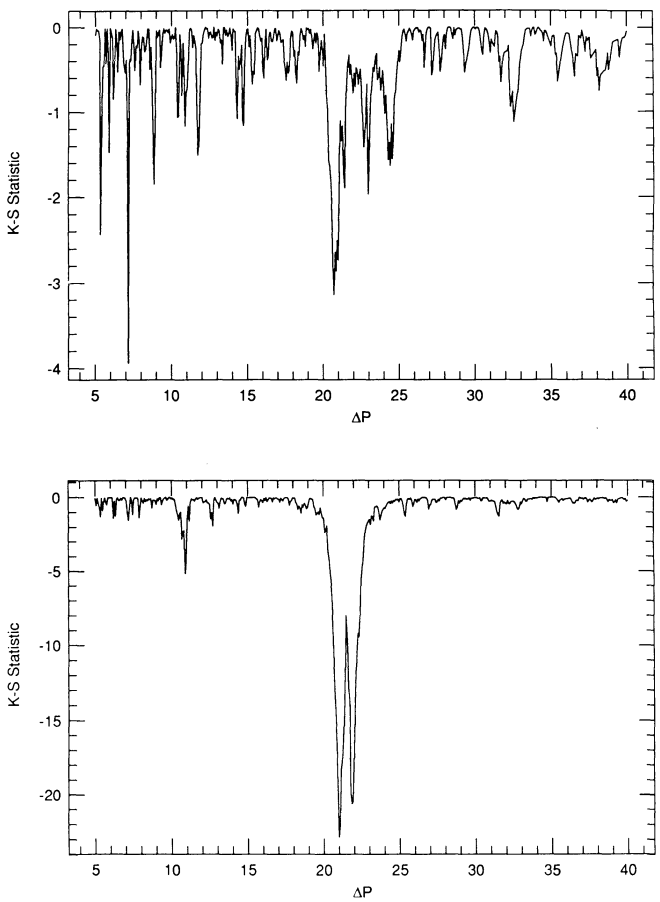

FIG. 8.—Kolmogorov-Smirnov (KS) test applied to the periods identified in PG 1159−035 for the unresolved data from single-site runs (*upper panel*) and from the periods identified in Table 3 (*lower panel*).

the $l = 2$ spacing; no correction is necessary for the $l = 1$ modes because their amplitudes are much more symmetric.

The observed ratio of the mean period spacings is then

$$\Delta P_{l=1}/\Delta P_{l=2} = 21.5/12.5 = 1.72 ,$$

while the ratio expected from theory is $\sqrt{3} \approx 1.73$.

Conspicuous by its absence in either the PT analysis or the KS test is any feature corresponding to $l = 3$ (i.e., a multiplet with seven peaks). Based on the observed ratios for $l = 1$ and $l = 2$, we would expect to find a period spacing near 8.8 s. If we inspect Figure 7 for a peak at this spacing, we find nothing at all—the expected value is actually a *minimum* in the transform. A similar conclusion follows from Figure 8. This agrees with what we expect based on the total power spectrum: we saw no isolated multiplets with more than five components, and none with splittings of 7.7 μHz (the value we would expect for $l = 3$). We conclude that the $l = 3$ multiplets, and higher, are not present in the data, to a limit set by the noise.

Now, following Kawaler (1986, 1987a, b, 1988), we are in a position to use the mean period spacings to determine the mass of the star. We have used a series of structure models, normalized to an evolutionary model, to develop a mass interpolation formula. The evolutionary model is an Iben 0.6 $M_\odot$ model with 10^{-2} $M_\odot$ surface helium layer (see Kawaler 1986, 1987b for a description). For the total stellar mass we have

$$\log (M/M_\odot) = -1.041 \log \{\Delta P_l[l(l+1)]^{1/2}\} + 1.312 .$$

We have tested the accuracy of this interpolation formula, and find that the interpolation error is of order $0.1(|M/M_\odot - 0.6|)$, which is negligible in this case.

From the $l = 1$ period splitting, we get $M/M_\odot = 0.587 \pm 0.003$, and from $l = 2$ we get $M/M_\odot = 0.582 \pm 0.003$. If we take the average of the two values, weighted by the number of modal intervals present in each, we find

$$M/M_\odot = 0.586 \pm 0.003 .$$

The stated error reflects only the uncertainty in the measured period spacings; we cannot yet assess the value of any systematic error which might arise from applying them to models whose physical conditions, composition, etc., do not accurately reflect those actually present in the star.

5.2.2. *Deviations from Uniform Period Spacing*

Deviations from uniform period spacing between successive multiplets in the theoretical models are the result of the effect of mode-trapping in the envelope. This occurs in a compositionally stratified model when there is a reasonance of a pulsation mode with a surface layer; the resonance occurs when radial nodes in a pulsation eigenfunction coincide with a layer boundary. Important practical examples of such layer boundaries in white dwarf models are transition zones between hydrogen and helium, or between helium and carbon/oxygen when stratification has been introduced to model the process of gravitational settling.

We can see the effect of different chemical stratifications on the period spacing in Figure 9, where we plot $\Delta P = (P_{k+1} - P_k)$ versus P_k for $l = 1$, 2 from the theoretical results of Kawaler (1987b) for three models with $\log L/L_\odot = 2.0$, and $M/M_\odot = 0.6$. These are: a homogeneous ^{12}C model, a model with a 10^{-2} $M_\odot$ layer of helium over a ^{12}C core which we refer to as He/C, and one with a 10^{-4} $M_\odot$ hydrogen layer on top of a 10^{-2} $M_\odot$ helium layer over a carbon core (H/He/C). Rotation was not specifically included in Kawaler's calculations

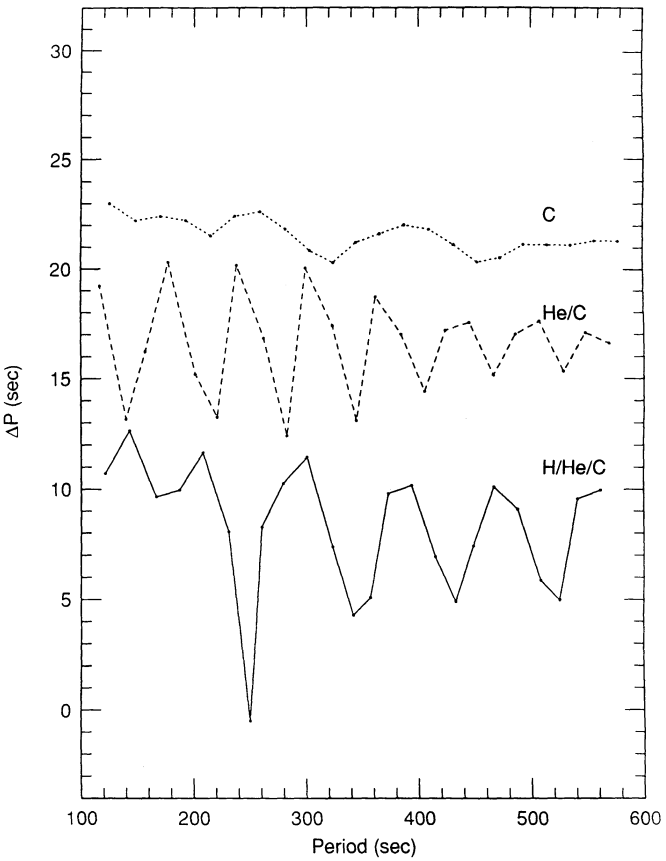

FIG. 9.—Theoretical period spacings (for $l = 1$ modes) for three different models, displaced vertically for clarity.

but, since $m = 0$ modes are not affected by rotation, we may still use his period spacings for any chosen l.

From the high-resolution power spectrum of the WET data set, we were able to identify twenty $l = 1$, $m = 0$ modes in PG 1159−035. Ten of these modes are the high-amplitude modes listed in Table 3 (and most are readily apparent in Fig. 4). Given these, we used the mean period spacing to identify a limited range in which to search for additional $l = 1$ modes; we were able to identify 10 additional modes by this procedure. Some of these are tentative identifications and are so indicated in Table 3. For each of the modes where there was some ambiguity, we divided that data into two halves and chose the peak that appeared in the same location in both halves. In addition to $l = 1$ modes, we have nine $l = 2$ modes which are nearly consecutive (two modes are missing).

In Figure 10 we plot the period spacing as a function of period for the observations of PG 1159−035. We have plotted the difference of each pair of periods, ΔP, against the lowest period mode (forward difference). This choice is arbitrary, although we have avoided the obvious choice of plotting the difference against the average period in order to retain the horizontal axis value as an observed quantity. The most striking feature of these curves is that they show the period spacings between consecutive modes (of a given l) deviate from the mean in a regular, and almost periodic, manner.

5.2.3. *Probing the Stellar Interior*

Immediately striking is that Figure 10 bears great qualitative resemblance to the theoretical plots in Figure 9. We will focus

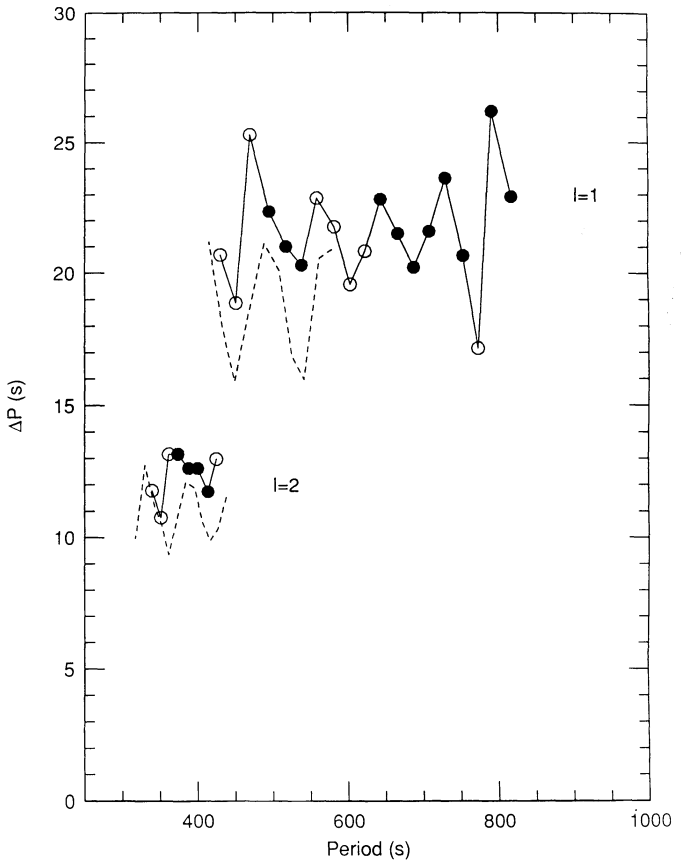

FIG. 10.—Observed period spacings in PG 1159−035. Open circle values are less certainly determined than those for the solid circles. The dashed lines show the theoretical trapping found in the H/He/C model. A small decrease in the model's mass would displace the dashed curves upward.

our comparison on the $l = 1$ modes, because we have much more observational information on their period spacing. We can characterize the spacing, in both the observations and the theoretical models, by fitting a sinusoid to the discrete values in Figures 9 and 10. We will call the period of this fitted sinusoid the trapping cycle period, and we can also derive an amplitude and a period of first minimum for the fit.

Before fitting, we divided the ΔP values by the mean period spacing for each model and the observations, and then subtracted one, so that the values were normalized and the mean was zero—much the same way we treated the original light curves. This procedure reduced the sensitivity to stellar mass for comparison with the theoretical models; the surface stratification becomes the dominant effect. In Table 4 we list the results for the three models of Kawaler (1987b) and for the observed quantities for PG 1159−035.

Comparing the theoretical versus observational parameters listed in Table 4 leaves little doubt that PG 1159−035 is compositionally stratified: none of its parameters are consistent with the chemically homogeneous model. In order to decide which of the two stratified models may provide the better fit, and how we might proceed to construct a model which would provide an even closer fit, we must know how the three trapping parameters are affected by the model structure.

The trapping cycle period is most sensitive to the thickness of the surface trapping layer, because the region of period formation for these high-overtone modes is primarily in the outer

TABLE 4

ΔP VERSUS P FIT RESULTS

Object/Model	Trapping Cycle (s)	Fractional Amplitude	T_{min}	$\langle \Delta P \rangle$
C.....	143 ± 7	0.030 ± 0.006	466 ± 9	21.2
He/C.....	63 ± 1	0.09 ± 0.01	528 ± 2	20.7
H/He/C.....	85 ± 1	0.18 ± 0.01	515 ± 1	18.5
PG 1159−035.....	80 ± 2	0.12 ± 0.02	523 ± 3	21.6

envelope. If we examine how the eigenfunctions change from mode to mode, we find that most of the change occurs in the outer layers. The more massive the layer, the deeper the composition transition zone, and so more modes are encountered after one trapped mode before the eigenfunction is altered sufficiently to create another resonance; that is, longer trapping cycles are associated with thicker regions of uniform composition. This is the reason the trapping cycle is longer for the chemically homogeneous model (where the trapping is the result of the relatively deep degeneracy boundary) than for the He/C model, or the H/He/C model.

By the same token, the H/He/C model has a longer trapping cycle than the He/C model—even though its outermost H-layer is thinner—because the trapping is the result of a double resonance in the eigenfunction with the two layers. The agreement between the observed trapping-cycle period and the H/He/C model (80 vs. 85 s) leads us to conclude that the envelope consists of two layers of differing chemical compositon—probably H/He, but a He/C layering cannot be ruled out. In any case, PG 1159−035 is obviously not a chemically homogeneous star.

The second parameter we consider is the trapping cycle amplitude. This is most sensitive to the density gradient in the composition transition zone: the larger the gradient the larger the trapping amplitude, a result of the change in the mean molecular weight. Here the observed amplitude (0.12) lies between the H/He/C value (0.18) and the He/C value (0.09). This suggests that the density gradient in the star is not as steep as in the H/He/C model, but steeper than the He/C model. The model would agree better with the observations if its helium layer contained a substantial amount of C/O, if its outermost layer were close to solar composition, or some mixture of these two effects.

The agreement of the local period of minimum (the most trapped mode in a specific period range) with the observed minimum period spacing is also a function of the number and thickness composition layers, as well as the total mass of the star. The relatively good agreement does suggest that the k value for the 516 s period triplet must be $k = 20 \pm 2$.

The tantalizing success of even this preliminary comparison with existing theoretical models serves, at the very least, to make clear the potential of the method; by careful model construction and matching we should be able to determine uniquely the compositional profile of the star.

5.3. *The Phase of the* 516 s *Period*

The 516 s period (1938 μHz frequency) appeared in the analysis of Winget *et al.* (1985) as a singlet, and its time of maximum was observed to undergo a parabolic change with time in the $(O-C)$ diagram. This change was consistent with the change expected from secular evolution (Winget, Hansen, & Van Horn 1983). Winget & Kepler (1988) showed that the

phase of the 516 s period was reasonably consistent with the previous ephemeris of Winget et al. (1985) despite the appearance of several new bands of power in 1987.

Now that we have resolved the band of power at 1938 μHz, we find that it is composed of a triplet of frequencies, with the previously studied period at 516 s appearing as the $m = +1$ component; the two other members of the triplet, if present at all, were of sufficiently low-amplitude until 1987 that they had little or no effect on the apparent phase and frequency of the band. We can now take this new identification into account in comparing these latest observations with the emphemeris.

In Figure 11 we plot the $(O-C)$ diagram of all available data on PG 1159−035, including the data from 1987. The solid line in the figure is the ephemeris from the 1985 fit—that is, based only on the first four data points—using the definitions of Winget & Kepler (1988):

$$dP/dt = (-2.4 \pm 0.4) \times 10^{-11} \text{ s s}^{-1} .$$

As we can see from the figure, the earlier fit passes right through the new 1989 data. The best $(O-C)$ values for each year are listed along with their errors in Table 5. The relatively large error associated with the point from 1987 arises primarily because the 516 s period was not well-resolved in the data set. It is also likely that the other triplet members, with 517 and 518 s periods, had already grown to small but significant amplitude. We conclude that even though these new pulsation modes appeared and shared power with the 516 s pulsation,

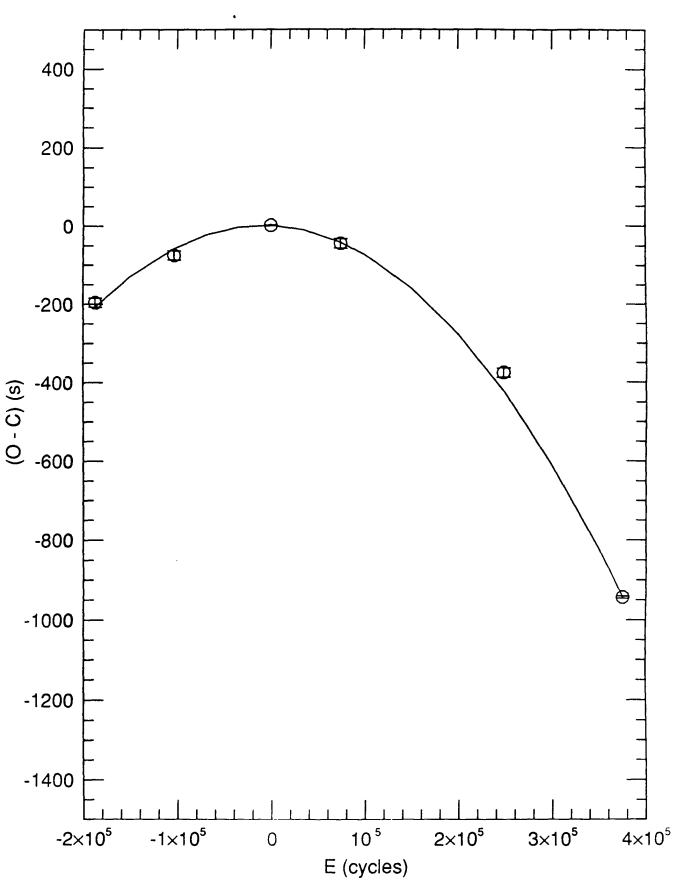

FIG. 11.—Observed phase of the 516 s period as a function of time (*circles*) with formal error bars shown. The solid curve is the phase ephemeris derived from the first four data points.

TABLE 5

SEASONAL $(O-C)$

Year	E(cycles)	$(O-C)$ (s)	$\sigma(T_{max})$ (s)
1979.....	−187009	−196	12
1981.....	−103345	−76	12
1983.....	0	0.6	1
1984.....	74300	−45	12
1987.....	248290	−375	24
1989.....	374992	−940	3

the phase of the latter remained constant except for the slow parabolic change ascribed to secular evolution (Winget et al. 1985), and the fit to the old ephemeris remained well within observational error.

The time of maximum obtained in 1989 can be used to refine our measurement of dP/dt by fitting a parabola to the $O-C$ results obtained excluding the $\dot{P}$ term in the following (Winget 1988a):

$$(O-C) = T_{\max}^{\text{obs}} - T_0 - P \cdot E - \frac{P}{2} \dot{P} E^2 ,$$

where E is the number of cycles which have elapsed since T_0 (Table 5).

With the new fit, we obtain

$$T_0 = (2445346.873562 \pm 0.000017)\text{BJDD} ,$$

$$P = 516.02531 \pm 0.00006 \text{ s} ,$$

$$dP/dt = (-2.49 \pm 0.06) \times 10^{-11} \text{ s s}^{-1} .$$

This latest result is consistent with, but more accurate than, the 1985 result.

5.4. *Mode Identification and the Derived Stellar Parameters*

Many of the parameters we have derived for this star are affected directly by our ability to assign the correct values of l, k, and m to the peaks in the observed power spectrum, but they are not all equally sensitive to them. The value of dP/dt, for example, is independent of modal assignments: it depends only on our ability to resolve a peak from its immediate neighbors and measure how its phase changes with time. Similarly, the limit to the magnetic field depends on the relative equality of the frequency splitting within a multiplet, not on the modal values assigned to it.

The derived mass and rotation period depend primarily on the correct assignment of the pulsation order, l. We have therefore applied three separate test procedures to confirm our assignments, and all three show that it is correct:

1. We derived the average splitting within multiplets identified as $l = 1$ separately from those identified as $l = 2$, and showed that the ratio of their frequency differences,

$$\frac{4.22 \ \mu\text{Hz}}{6.91 \ \mu\text{Hz}} = 0.61 ,$$

agrees with the ratio of 0.60 expected from theory.

2. We developed a period transform of the power spectrum (PT) covering the full region of our analysis, so we could see if its Fourier transform displayed the effects of multiplet separations equally spaced in period, as predicted by the theory in its asymptotic approximation for large k. It does (see Fig. 7). The ratio of the mean period spacings derived from the two signifi-

cant peaks in this transform,

$$\frac{21.5\ \text{s}}{12.5\ \text{s}} = 1.72\ ,$$

agrees with the theoretical ratio of 1.73.

3. We then applied the K-S test to the peaks we had identified as significant (given in Table 3), after all of the "alias peaks" had been identified and removed. The result agreed with the PT test, showing that our modal assignments were basically correct, and displayed an improved signal-to-noise ratio (Fig. 8).

We are therefore confident of our l-mode assignments, and of the derived stellar parameters that are most sensitive to them.

The unambiguous identification of the m values was not possible in all cases, as Table 3 shows. On occasion we found that two peaks in a multiplet were of large amplitude while the other possible companions were small, and it was difficult to decide if a small peak on the high-frequency side was the correct companion, or one on the low-frequency side. Such small uncertainties are not serious, however, nor is our ability to assign a precise k value to a given multiplet. The only part of the analysis that depends on m and k values involves our identification of a chemically stratified model as the best-fit to the period spacing data (Fig. 10). Even if we discard all of the uncertain points, the individual fitting parameters change somewhat, but the identification of the chemically stratified model as the best fit remains unchanged.

6. OLD MODELS AND NEW MYSTERIES

We now address those results which we cannot describe on the basis of existing theory or simple extensions of it.

6.1. *New Bands of Power*

Koupelis & Winget (1987, hereafter KW) noted that new bands of power had appeared in the 1987 optical and X-ray data of PG 1159−035 that were not detectable in the earlier (1979–1984) data set of Winget et al. (1985). Their centroids had periods of approximately 560, 524, 508, and 414 s.

We have searched for new bands of power in the WET data and find nothing new with large amplitude. We have found many new bands showing low-amplitude signals, but these are readily explained by the increased sensitivity in the WET instrument. Moreover, two of the bands reported by KW near 524 and 508 s are significantly absent in our data set.

The relevant portion of the power spectrum of the WET data is shown in Figure 12, together with a simulated power spectrum containing only the six frequencies corresponding to the 516 and 539 triplets, in mirror image. The power in the vicinity of the 524 and 508 s regions is completely accounted for by power in the sidelobes of the two triplets; there is no excess power. Both of these peaks, based on period spacing considerations, are certainly not $l = 1$ modes but could be $l = 2$ modes.

Interestingly, the 560 s period is still present, at roughly the same level as in 1987, and clearly is an $l = 1$ triplet. The 414 s structure is also still present, and is consistent with an $l = 2$ group. It appears to be at a lower amplitude in 1989 than in 1987, but the 1987 data are from a single longitude and do not resolve the structure, so the comparison may not be meaningful.

6.2. *Stability of Mode Structure*

The comings—and possibly goings—of power in the pulsation spectrum of PG 1159−035 are marked by one constant factor: in the decade of observations of this star, the basic

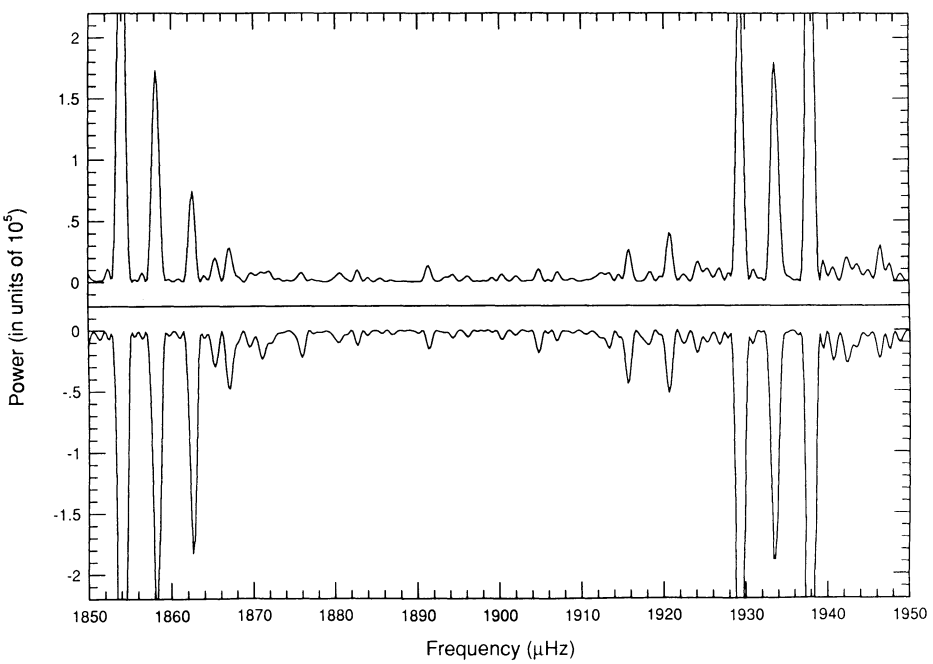

FIG. 12.—Power spectrum in the region of the 524 and 508 s periods (*upper curve*) together with the spectral window formed from the 516 and 539 s triplets only (*lower curve, reverse image*). They account for all of the observed power.

underlying mode structure, which we have uncovered in these latest observations, has remained the same.

Our data are consistent with no change in the frequency locations of the original eight bands of power reported by Winget et al. (1985). We now know that the previously unresolved character of these bands is due to rotational splitting of nonradial g-modes with sperical harmonic indices of $l = 1$ and $l = 2$. The new modes reported by Koupelis & Winget (1987) are consistent with modes of the same l values, but with k values different from the modes previously observed. The underlying mode structure has apparently remained the same throughout the observations, and the new modes have simply grown to detectable amplitude without any alterations in their frequencies.

The same point can be made about the additional power discovered in this investigation in the vicinity of the 516 s ($m = +1$) mode. The two new frequencies are simply the $m = -1$ and $m = 0$ components of this $l = 1$ triplet and were not previously excited to observable amplitude. This stability of the underlying frequency structure, coupled with the remarkable stability of the secular phase variations in the 516 s mode, argues that the observed changes are not the result of substantial changes in the structure of PG 1159−035, but could be the result of more subtle changes in the driving region.

6.3. *Conservation of Power Near the* 516 s *Mode*

From the standpoint of nonlinear theory, perhaps the most interesting and approachable result of the new data set relates to the presence of this new power near the 516 s period. Power appeared as a well-isolated singlet in the data set of Winget et al. (1985); the stability of its fractional amplitude from run to run indicated that if there were any nearby periodicities their fractional amplitudes were less than 10% of the amplitude of the 516 s mode.

The surprise came from the 1989 WET data reported here. What had been a 516 s singlet, as shown from a lack of beating with any nearby periodicities, was now *very* conspicuously a triplet: 516.04, 517.18, and 518.32 s with fractional amplitudes of, respectively, (6.9, 4.2, and 5.1) $\times 10^{-3}$. Had these additional members of the triplet been present at these amplitudes in the earlier data, conspicuous beating effects would have been noticed.

Most interesting is the result that power was conserved as the two new modes appeared. They apparently arose at the expense of the $m = +1$, or prograde, mode at 516 s: the square root of the sum of the power of the three modes in the 1989 WET data is 9.56×10^{-3}, to be compared with the 1983 value of 9.59×10^{-3}.

This result poses an extremely interesting theoretical problem, because the energy transfer time scale is intimately related to the growth rates for the modes in a weakly dissipative system. The problem should be a straightforward one to solve—indeed, it may be the only nonlinear problem related to any of these variable white dwarfs which is currently solvable; three nearly commensurate frequencies (within 0.2% of each other) swap power with the total power conserved. We note that theoretically we would expect such a conservative transfer to be periodic rather than secular, although we do not yet have enough evidence to decide on observational grounds.

6.4. *Amplitudes and Mode Trapping*

The amplitude of a given mode is related monotonically (but not linearly) to its growth rate (Dziembowski 1988; Buchler 1988). This relationship has led to the speculation in the literature that modes with the largest observed amplitude are probably the modes with the fastest growth rates. In the absence of any significant mode selection mechanism due to nonadiabatic processes, the modes with the fastest growth rates should be those which are trapped in the outermost layers and thus, by the above argument, have the largest amplitudes (Winget, Van Horn, & Hansen 1981; Dolez & Vauclair 1981; Winget & Fontaine 1982).

As we have seen, we can identify the trapped modes in this star as those having the smallest period spacing relative to the mean. If we compare the amplitudes of the trapped and untrapped modes (using Table 3 and Fig. 10) we see no clear relation between trapped modes and the modes of highest amplitude; that is, we do not find the expected correlation between mode trapping and observed amplitude of the mode. If this result is not wavelength-dependent, we are then forced to conclude that the magnitude of the growth rate is *not* directly related to mode trapping in the envelope.

In any case, we conclude that although mode-trapping definitely occurs in PG 1159−035—and therefore probably in the other DOV stars as well—it is not possible to identify the trapped modes based only on optical pulsation amplitudes; we must have period spacing data to identify them.

6.5. *Growth Rates as a Function of m and k*

Theoretical investigations of the effects of slow rotation on the growth rates suggest that we would expect very little difference in the physical amplitude of modes within a given multiplet, with perhaps some systematic enhancement of the prograde modes (Carroll & Hansen 1982; Hansen, Cox, & Carroll 1978). This result agrees with our intuitive expectation that modes of a given multiplet have frequencies so close together (in the slow rotation case applicable here) that the radial dependence of their eigenfunctions must be similar. From very similar pulsation time scales and very similar eigenfunctions we would expect very similar growth rates. The observed amplitudes within a multiplet should then be due mostly to inclination effects, so we would expect to see amplitude distributions within a multiplet which are roughly symmetric about $m = 0$, with perhaps slightly larger amplitudes for the prograde modes. This pattern should be very insensitive to the value of k, and the average of both $l = 1$ and 2 should yield the same inclination. For the first time we have an opportunity to test our expectations for a compact pulsator; they are wrong.

The amplitudes of the modes within each multiplet are very different in most cases, and generally are very asymmetric. Further, they differ dramatically with k for both $l = 1$ and $l = 2$. For the $l = 1$ modes the *average* is nearly symmetric about zero, and we can derive an inclination from it—but with caution, considering that the $l = 2$ average is still very asymmetric.

Our results do imply that the amplitude (and hence probably also the growth rate) is a function of m as well as l and k. Therefore this function is more complicated than just uniformly enhancing the prograde or retrograde modes as we might naïvely expect.

6.6. *dP/dt and* $P_{\rm rot}$

The new data reported here confirm both the magnitude and the negative sign of the rate of period change seen in the 516 s periodicity. Both are in excellent agreement with the theoreti-

cal expectations of Winget, Hansen, & Van Horn (1983, hereafter WHVH). They showed that secular evolution produces a negative rate of period change which is a combination of two principal effects: gravitational contraction—tending to decrease the period, and cooling—tending to increase the period. They found that the rate of period change should eventually become positive, as contraction was slowed by degeneracy, but not until luminosities decreased to well below the observed luminosity of PG 1159−035 ($\log [L/L_\odot) \approx 2$].

The WHVH calculations used evolutionary models with the best available treatment of the interior, envelope equation of state and opacities for their pulsation calculations. However, the models used to start the evolutionary sequences were polytropes, not models which had evolved through prior stages of nuclear burning. They reached the vicinity of PG 1159−035 in the H-R diagram via gravitational contraction and heating along a roughly constant luminosity track, in the position of the observed extended horizontal branch (EHB) stars (see Winget & Cabot 1980).

Kawaler, Hansen, & Winget (1985) and Kawaler (1986) repeated the calculations using the hot cores of evolutionary asymptotic giant branch stars as initial models. The envelope mass was stripped away artificially to imitate the observed mass-loss in order to produce models appropriate to a planetary nebula nucleus (hereafter PNN). They found that dP/dt was *always* positive to cooling PNN model with $\log (L/L_\odot) \lesssim 3$. This result held for *any* models constructed in this way; the result was extremely insensitive to total stellar mass, layer mass and composition, nuclear shell burning, or core composition. All of these models therefore disagreed with the observations.

Kawaler et al. (1985) proposed a solution to this dilemma: they noted that if the 516 s pulsation was an $l = 2$ or 3 mode with $m = l$ (the prograde sectoral mode), then the sign of dP/dt might be determined by the spin-up associated with evolutionary contraction. This required a rotation period shorter than about 3000 s, in order to reverse the sign of dP/dt for their post-PNN models. Given the rotation period we have derived from the observations, $P_{\rm rot} = 1.38$ days, this possibility can now be ruled out.

The only obvious alternatives are that the secular change in frequency does not measure the actual cooling rate, and therefore the good agreement of its value with that predicted by cooling theory is a coincidence, or that the progenitor of PG 1159−035 is substantially different from the immediately post-planetary models of Kawaler (see the discussion in Kawaler 1986). Perhaps it evolved along the EHB, similar to the models of Winget, Hansen, & Van Horn (1983).

This problem clearly deserves further theoretical attention, especially since we should be able to determine the compositional structure by matching the period variations with k as described above. It seems that if we can match both the period structure and the value of dP/dt we should be able to identify the nature of the progenitor to PG 1159−035.

7. SUMMARY

Our most fundamental observational result is the large number of resolved frequencies present. To within our ability to detect and identify them, they consist entirely of two distinct sets of multiplets corresponding to quantized pulsations of the lowest two orders, $l = 1$ and $l = 2$. The period spacing between the multiplets, the uniform frequency spacing within the multiplets, and the number of components in the multiplets lead directly to their individual identifications, and allow us to derive unique physical values for many important stellar parameters.

We summarize our results below, but caution that many questions still remain, both observational and theoretical, concerning this star and other variable white dwarfs. We are gratified that these are new puzzles, however, because we now seek answers to questions we were not even able to ask before. First, the basic pulsation results:

1. Most, and probably all, of the observed variations in the star are due to nonradial g-mode pulsations.
2. Slow rotation is responsible for the fine-structure multiplets.
3. Asymptotic theory (in the high radial overtone limit) provides a very accurate description of the observed frequencies and their distributions.
4. Only modes with spherical harmonic index $l = 1$ and $l = 2$ are detected. There is no evidence for pulsations with $l = 3$ or higher.
5. We have identified 101 modes to which we can assign unique values of l and m, and the radial overtone number k is contrained from theory to within $\sim \pm 2$.
6. Physical amplitudes vary with m within a multiplet, but not in any obvious systematic way with k.
7. Mode trapping via compositional stratification can account for the variations in period spacing between consecutive modes of like l.
8. Amplitude is not a good predictor of mode trapping.

Next, we list the stellar parameters we have determined or constrained on the basis of a preliminary seismological analysis using published theoretical models:

1. The seismological mass of PG 1159−035 is 0.586 ± 0.003 $M/M_\odot$.
2. The inclination to our line of sight is 60°.
3. This prewhite dwarf star is already a slow rotator. The rotation period is 1.38 ± 0.01 days.
4. The magnetic field of the star is $B \lesssim 6000$ G.
5. The star is compositionally stratified.

Computing a grid of theoretical models with a range of surface layer compositions and core compositions may allow us to determine uniquely the chemical structure of the star. This information can be coupled with the value of dP/dt measured for the 516 s period, and the values we expect to obtain for the other large-amplitude pulsations, to yield a remarkably complete understanding of both its structure and evolution.

The information we have obtained about fundamental parameters of the star PG 1159−035, even in this preliminary form, demonstrates the potential for the application of the observational and theoretical tools of asteroseismology. Many of the parameters cannot be measured in any other way. We are confident that asteroseismology will take its place along with stellar atmospheres (and its observational partner, spectroscopy) as one of the primary ways in which stars are studied.

We are grateful for support from NSERC Canada, CNRS France, SERC UK, the National Science Foundation grants AST85-52456, AST86-00507, AST87-12249, AST88-13572, NASA grant NGT-50210 and from the National Geographical Society grant 3547-87.

APPENDIX

In the slow rotation limit, (i.e., $\Omega_{\rm rot} \ll \sigma_{kl}$), the frequencies are given by

$$\sigma_{klm} = \sigma_{kl} + m(1 - C_{kl} - C'_{klm})\Omega + O(\Omega^2)\,, \tag{1}$$

where the last term indicates terms of second-order in the rotation frequency, Ω; C_{kl} is an integral of the eigenfunctions over the star and is the contribution from uniform rotation; C'_{klm} is the contribution due to differential rotation, which depends only on the absolute value of m (see Hansen, Cox, & Van Horn 1977); and finally, σ, with its various subscripts, is the angular pulsation frequency where $\sigma = 2\pi\nu$. In the asymptotic limit of high radial overtone (certainly valid here where $k \gtrsim 20$, Kawaler 1988), the uniform rotation contribution to splitting is

$$C_{kl} \simeq \frac{1}{l(l+1)}\,, \tag{2}$$

which is independent of k. Thus, in the asymptotic limit, with uniform rotation, and keeping only the terms linear in Ω, we have for the ratio, R, of the rotational splittings for $\Delta m = 1$,

$$R_{1,2} = \frac{\delta\sigma_{l=1}}{\delta\sigma_{l=2}} = \frac{\delta\nu_{l=1}}{\delta\nu_{l=2}} = \frac{(1 - C_{k1})}{(1 - C_{k2})} = 0.60$$

which is also independent of k.

We have investigated the effects of nonuniform rotation by using a variety of rotation laws. These include "rotation on cylinders" as applied by Hansen et al. (1977) (and see Cuypers 1980), and spherically symmetric laws (with Ω a function of radius only; see Unno et al. 1989, § 19.2). For the latter, $\Omega(r)$ was chosen to be a maximum at stellar center and to decrease as a Gaussian outward in radius; various half-widths for the Gaussian were considered. The surprising result, as applied to a DOV PG 1159 model, is that the ratio $R_{1,2}$, as computed by direct integration of all the integrals implicit in equation (1), deviates only slightly from its uniform rotation limit of 0.60 provided that k is large (greater than about 5). The reason for this is that eigenmodes of large k look very much the same independent of k (where just the overall number of nodes change). The k-independent result for $R_{l,l'}$ can also be shown analytically in the same way as equation (2) is derived.

We conclude that our observations are not very sensitive to the many possible kinds of rotation laws, so long as we observe stars that show only large values of k. We expect the DBV and DAV stars to exhibit far smaller k values, and there we should be much more sensitive to the rotational processes the stars exhibit.

REFERENCES

Barstow, M. A., & Holberg, J. B. 1989, in Extreme Ultraviolet, ed. R. F. Malina, & C. S. Bowyer (Oxford: Pergamon), in press
Barstow, M. A., Holberg, J. B., Grauer, A. D., & Winget, D. E. 1986, ApJ, 306, L25
Buchler, R. 1988, in Workshop Proceedings, Multimode Stellar Pulsations, ed. G. Kovács, L. Szabados, & B. Szeidl (Budapest: Konkoly Observatory), 71
Carroll, B. W., & Hansen, C. J. 1982, ApJ, 263, 352
Cox, A. N. 1987, in IAU Colloquium 95, The Second Conference in Faint Blue Stars, ed. A. G. D. Philip, D. S. Hayes, & J. Liebert (Schenectady: Davis Press), 631
Cox, J. P. 1984, PASP, 96, 577
Cuypers, J. 1980, A&A, 89, 207
Dolez, N., & Vauclair, G. 1981, A&A, 102, 375
Dziembowski, W. 1988, in Workshop Proceedings Multimode Stellar Pulsations, ed. G. Kovács, L. Szabados, & B. Szeidl (Budapest: Konkoly Observatory), 127
Hansen, C. J., Cox, J. P., & Carroll, B. W. 1978, ApJ, 226, 210
Hansen, C. J., Cox, J. P., & Van Horn, H. M. 1977, ApJ, 217, 151
Iben, I. Jr., & Laughlin, G. 1989, ApJ, 341, 312
Jones, P. W., Pesnell, W. D., Hansen, C. J., & Kawaler, S. D. 1989, ApJ, 336, 403
Kawaler, S. D. 1986, Ph.D. thesis, University of Texas
———. 1987a, in Stellar Pulsation, ed. A. N. Cox, W. M. Sparks, & S. G. Starrfield (Berlin: Springer), 367
Stars, ed. A. G. D. Philip, D. S. Hayes, & J. Liebert (Schenectady: Davis Press), 297
———. 1988, in IAU Symposium 123, Advances in Helio- and Asteroseismology, ed. J. Christiansen-Dalsgaard & S. Fransden (Dordrecht: Reidel), 329
Kawaler, S. D., Hansen, C. J., & Winget, D. E. 1985, ApJ, 295, 547
Koupelis, T., & Winget, D. E. 1987, in IAU Colloquium 95, The Second Conference on Faint Blue Stars, ed. A. G. D. Philip, D. S. Hayes, & J. Liebert (Schenectady: Davis Press), 623
McGraw, J. T., Starrfield, S. G., Liebert, J., & Green, R. F. 1979, in IAU Colloquium 53, White Dwarfs and Variable Degenerate Stars, ed. H. M. Van Horn & V. Wiedemann (Rochester, N.Y.: University of Rochester Press), 377
Nather, R. E., Winget, D. E., Clemens, J. C., Hansen, C. J., & Hine, B. P. 1990, ApJ, 361, 309
Pesnell, W. D. 1985, ApJ, 292, 238
Unno, W., Osaki, Y., Ando, H., Saio, H., & Shibahashi, H. 1989, Nonradial Oscillations of Stars (2nd. ed.; Tokyo: University of Tokyo Press)
Unno, W., Osaki, Y., Ando, H., Shibahashi, H. 1979, Nonradial Oscillations of Stars (Tokyo: University of Tokyo Press)
Wesemael, F., Green, R. F., & Liebert, J. 1985, ApJS, 58, 379
Winget, D. E. 1988a, in IAU Symposium 123, Advances in Helio- and Asteroseismology, ed. J. Christensen-Dalsgaard & S. Frandsen (Dordrecht: Reidel), 305
———. 1988b, in Workshop Proceedings Multimode Stellar Pulsations, ed. G. Kovács, L. Szabados, & B. Szeidl (Budapest: Konkoly Observatory), 181
Winget, D. E., & Cabot, W. 1980, ApJ, 242, 1166
Winget, D. E., & Fontaine, G. 1982, in Pulsations in Classical and Cataclysmic Variable Stars, ed. J. P. Cox & C. J. Hansen (Boulder: University of Colorado Press), 46
Winget, D. E., Hansen, C. J., Liebert, J., Van Horn, H. M., Fontaine, G., Nather, R. E., Kepler, S. O., & Lamb, D. Q. 1987, ApJ, 315, L77
Winget, D. E., Hansen, C. J., & Van Horn, H. M. 1983, Nature, 303, 781
Winget, D. E., Kepler, S. O., Robinson, E. L., Nather, R. E., & O'Donoghue, D. 1985, ApJ, 292, 606
Winget, D. E., & Kepler, S. O. 1988, in Workshop Proceedings Multimode Stellar Pulsations (Budapest: Konkoly Observatory), 205
Winget, D. E., & Van Horn, H. M. 1987, in IAU Colloquium 95, The Second Conference on Faint Blue Stars, ed. A. G. D. Philip, D. S. Hayes, & J. Liebert (Schenectady: Davis Press), 363
Winget, D. E., Van Horn, H. M., & Hansen, C. J. 1981, ApJ, 245, L33
Wood, M. A. 1990, JRASC, in press